Design, Synthesis, and Biological Evaluation of Novel Aminobisphosphonates Possessing an in Vivo Antitumor Activity Through a γδ-T Lymphocytes-Mediated Activation Mechanism

Daniele Simoni,*[,†] Nicola Gebbia,[‡] Francesco Paolo Invidiata,[§] Marco Eleopra,[†] Paolo Marchetti,[†] Riccardo Rondanin,[†]
Riccardo Baruchello,[†] Stefano Provera,[‖] Carla Marchioro,[‖] Manlio Tolomeo,[⊥] Luciana Marinelli,[#] Vittorio Limongelli,[#]
Ettore Novellino,[#] Aaron Kwaasi,[∇] James Dunford,[∇] Simona Buccheri,[○] Nadia Caccamo,[○] and Francesco Dieli[○]

*Dipartimento di Scienze Farmaceutiche, Università di Ferrara, Italy, Via Fossato di Mortara 17/19, 44100 Ferrara, Italy, Consorzio di
Ricerca sul Rischio Biologico in Agricoltura (Co.Ri.Bi.A.), Palermo, Italy, Dipartimento Farmacochimico Tossicologico e Biologico, Università
di Palermo, Italy, GlaxoSmithKline, Medicines Research Center, Via Fleming 4, 37135 Verona, Italy, Divisione di Ematologia e Servizio AIDS
Policlinico, Università di Palermo, Italy, Dipartimento di Chimica Farmaceutica e Tossicologica, Università di Napoli "Federico II", Via D.
Montesano, 49, 80131 Napoli, Italy, Nuffield Department of Orthopaedic Surgery, The Botnar Research Centre, University of Oxford, Institute
of Musculoskeletal Sciences, Nuffield Orthopaedic Centre, Headington, Oxford OX3 7LD, United Kingdom, Dipartimento di Biopatologia e
Metodologie Biomediche, Università di Palermo, Italy*

　　　　　A small series of aminobisphosphonates (N-BPs) structurally related to zoledronic acid was synthesized
　　　　　with the aim of improving activity toward activation of human γδ T cells and in turn their in vivo antitumor
　　　　　activity. The absence of the 1-OH moiety, together with the position and the different basicity of the nitrogen,
　　　　　appears crucial for antitumor activity. In comparison to zoledronic acid, compound **6a** shows a greater
　　　　　ability to activate γδ T cells expression (100 times more) and a proapoptotic effect that is better than zole-
　　　　　dronic acid. The potent activation of γδ T cells, in addition to evidence of the in vivo antitumor activity of
　　　　　6a, suggests it may be a new potential drug candidate for cancer treatment.

Introduction

Nitrogen-containing bisphosphonates (N-BPs),[a] a class of
geminal bisphosphonates (BPs), with **1** containing nitrogen in
the R_2 side chain, are important drugs widely used in a variety
of bone resorption diseases, such as osteoporosis, Paget's
disease, and hypercalcemia.[1] Some also have antiparasitic and
antibacterical activity.[2] They act by inhibiting the enzyme
farnesyl diphosphate synthase (FPPS),[3] which plays an important
role in the mevalonate pathway and in protein prenylation.[4]
Recently, N-BPs have gained additional importance as they have
been shown to inhibit tumor cell adhesion, invasion, and
proliferation and to induce apoptosis of a variety of human tumor
cell lines in vitro.[5] More importantly, N-BPs also have been
shown to exhibit direct antitumor activity in vivo by inhibiting
cancer growth through antiangiogenic, anti-invasive, and im-
munomodulatory actions.[6] Although several mechanisms have
been proposed to explain the N-BPs' antitumor effect, the
inhibition of FPPS surely plays an important role in their
anticancer properties. This inhibition results in the reduced
prenylation of a variety of proteins with mediator functions in

signaling cascades such as Ras2 or Rho. It also results in the
accumulation of isoprenoids, such as IPP (isopentenyl pyro-
phosphate), which induce expansion of γδ T cells. Nowadays,
there is substantial evidence that γδ T cells (which, in humans,
comprise only 5–10% of all circulating T-cells) possess potent
antitumor activities. They are capable of recognizing tumor
targets via cancer antigens or stress-induced molecules without
the requirement of classical MHC presentation. This gives broad
applicability across a large range of tumor types. Different
biological studies have demonstrated that γδ T cells are effective
against different types of cancer such as melanomas, renal
carcinoma, lymphoma, and multiple myeloma.[7] Thus, γδ T cells,
or γδ T cells agonists, such as N-BPs, could play a major role
in controlling human malignancy and could be used therapeuti-
cally in combination with other anticancer agents. Indeed,
clinical studies have recently shown that adding immune therapy
to classical chemotherapy has survival benefits when compared
to chemotherapy alone.[8] There is, therefore, major interest in
the development of novel N-BPs as new promising anticancer
agents.

Structurally, geminal bisphosphonates (BPs) **1** are analogues
of endogenous pyrophosphate in which a carbon atom replaces
the central atom of oxygen. This substitution makes BPs resistant
to hydrolysis and allows two additional chains of variable
structure. The ability of BPs to interact with specific molecular
targets strictly depends on the BP structural properties. For
example, it is well-known that acid phosphonic groups are
essential for high affinity for bone mineral, and that this is further
increased by the hydroxyl group at the side chain on central
carbon atom position ("bone hook").[9] Consequently, BPs such
as clodronate or etidronate, which represent the "first generation"
of BPs, are rapidly adsorbed by bone and therefore have been
primarily used in bone loss therapy. To increase the activity of
the above-mentioned drugs, a "second generation" of BPs, all
containing nitrogen (N-BPs), have been developed. These
include compounds such as pamidronate or ibandronate (Figure

* To whom correspondence should be addressed: Phone: 39-(0)532-
455923. Fax: 39-(0)532-455953. E-mail: smd@unife.it.
　† Dipartimento di Scienze Farmaceutiche, Università di Ferrara.
　‡ Consorzio di Ricerca sul Rischio Biologico in Agricoltura.
　§ Dipartimento Farmacochimico Tossicologico e Biologico, Università
di Palermo.
　‖ GlaxoSmithKline, Medicines Research Center.
　⊥ Divisione di Ematologia e Servizio AIDS Policlinico, Università di
Palermo.
　# Dipartimento di Chimica Farmaceutica e Tossicologica, Università di
Napoli "Federico II".
　∇ Nuffield Department of Orthopaedic Surgery, The Botnar Research
Centre, University of Oxford, Institute of Musculoskeletal Sciences, Nuffield
Orthopaedic Centre.
　○ Dipartimento di Biopatologia e Metodologie Biomediche, Università
di Palermo.
　a Abbreviations: N-BPs, nitrogen-containing bisphosphonates; BPs,
bisphosphonates; FPPS, farnesyl diphosphate synthase; IPP, isopentenyl
pyrophosphate; TBD, 1,5,7-triazabicyclo[4.4.0]dec-5-ene.
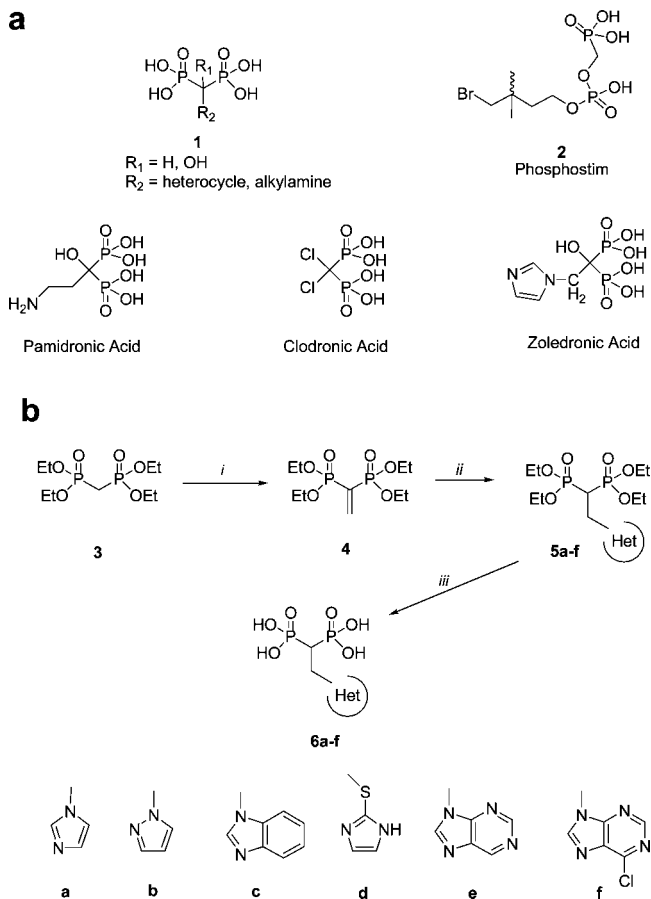
Figure 1. (a) General structures of geminal bisphosphonates (BPs) and structures of bisphosphonic acid reported in literature. (b) Synthesis of new bisphosphonates used in current study. Reagents and conditions: (i) Et$_2$NH, (CHO)n, pTSA; (ii) Het(a−f), TBD; (iii) HCl conc or TMSI.

1a). The mechanism of action of the first and second generations of BPs differs, as the former act by accumulating a toxic analogue of adenosine triphosphate,[10] while the latter lead to the inhibition of the FPPS. Indeed, the protonated-nitrogen forms of N-BPs closely resemble the cationic transition state/reactive intermediate formed during the FPPS catalytic cycle. This inhibition capacity of second generation N-BPs is also common to the "third generation" of N-BPs, which are essentially aromatic N-BPs and are extremely potent FPPS inhibitors. As mentioned above, the inhibition of FPPS is of crucial importance in the expansion and activation of $\gamma\delta$ T cells.[11] In this regard, Wilhelm et al.[12] reported the results of a pilot study of low-dose interleukin-2 (IL-2) in combination with pamidronate in patients with low-grade non-Hodgkin lymphoma or multiple myeloma. It has been shown that, of nine patients, five had significant in vivo activation/proliferation of $\gamma\delta$ T cells. Of these, three achieved objective responses, indicating that $\gamma\delta$ T cells are the main cell type responsible for the observed antilymphoma effect.

In line with this study, we first showed that zoledronic acid was as able as phosphoantigen isopentenylpyrophosphate (IPP) to induce expansion of $\gamma\delta$ T cells in vitro in the presence of IL-2.[13] Prompted by this finding, we decided to examine the feasibility and effects of using the $\gamma\delta$ T cells' agonist zoledronate alone or in combination with IL-2. We therefore began a phase I clinical trial in metastatic hormone-refractory prostate cancer. The results clearly show that administration of zoledronate together with IL-2 represents a novel, safe, and feasible

approach to inducing immunological and clinical responses in patients with metastatic carcinomas.[14]

Encouraged by such positive results and with the aim of finding more potent novel $\gamma\delta$ T cells agonists, we synthesized a small series of modified N-BPs structurally related to zoledronic acid (Figure 1b).

Chemistry. Bisphosphonates **6a−f** were prepared from a common starting intermediate, the methylenebisphosphonate **4**, by treatment with the proper heterocyclic nucleophile as shown in Figure 1b. TBD (1,5,7-triazabicyclo[4.4.0]dec-5-ene) was used as the catalyst. Additionally, bisphosphonate derivatives were also prepared from the corresponding methylenebisphosphonate **4** by treatment with the proper nucleophile at 150−160 °C for 15 min in a scientific microwave oven. The bisphosphonate acid derivatives **6a−f** were in turn obtained, starting from the corresponding ester derivatives, by treatment with hydrochloric acid or with iodotrimethylsilane. Compound **6e** has been fully studied by means of NMR techniques to determine the regioisomery of the major resulting structure. Peaks assignments were achieved for both isomers, directly on the 90:10 mixture, using gHMQC and gHMBC experiments, while gROESY experiments allowed the determination of the chain position. Related results should also be valid for compound **6f**.

Results and Discussion

Molecular Modeling. In the design of the novel compounds, we benefited from the recent three-dimensional pharmacophore model developed by Oldfield et al., who identified hydrophobic, aromatic, and cationic features, together with two metal-binding groups, for the creation of a BP with antitumor activity.[15] We also began with the knowledge of how our lead (zoledronate) binds to the FPPS catalytic site. In analyzing the details of the interactions between zoledronate and the FPPS catalytic site (PDB codes of the X-ray structures: 1ZW5, 2F8Z, 2F9K), it emerges that the two phosphonate groups are highly important for the binding of zoledronate to the enzyme. This is because they are responsible for the coordination of the three metal ions present in the FPPS active site. Even the imidazole moiety of zoledronate plays an important role in the binding to the enzyme. Indeed, the imidazole in its protonated state mimics the carbocation intermediate formed during the catalysis, and the protonated nitrogen makes a double H-bond with the Lys200 carbonyl oxygen and the Thr201 side chain (O$^\gamma$1). As a consequence, the only group that could be substituted without a dramatic decrease of the FPPS inhibition would be the 1-OH group, which, in the binary complex FPPS-zoledronate, forms a H-bond with Asp243. Here, to test our hypothesis, we performed molecular docking studies of zoledronate and 1-deshydroxyzoledronate (**6a**) using the FPPS (PDB code: 2F8Z) as receptor. As expected, docking calculations provided a binding mode of **6a** largely overlapping with that of zoledronate. Furthermore, the computed binding free energy of **6a**, −10.8 kcal/mol, is comparable to that of zoledronate, −9.8 kcal/mol, within the statistical error of the algorithm used for docking. The only difference in the binding mode of **6a** with respect to zoledronate resides in the lack of the interaction established by the hydroxyl group, which is absent in **6a**.

If the removal of the 1-OH does not substantially influence the inhibition of FPPS, it should have a certain impact on zoledronate activity in vitro and especially in vivo. In fact, removal of this group should reduce the bone and the skeletal retention and should increase exposure of the drug in the peripheral blood and in the soft tissue with an increase in the
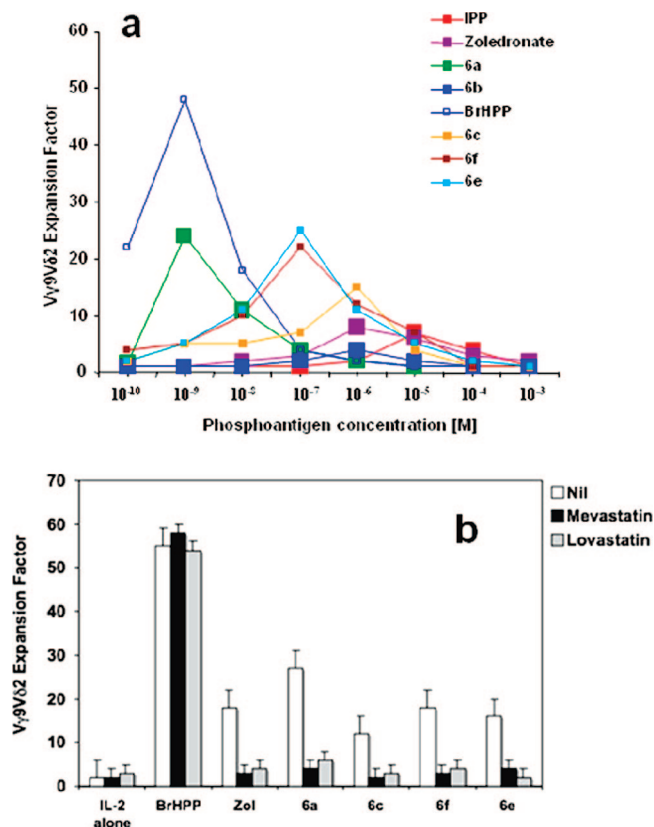
Figure 2. (a) Ability of different N-BPs derivatives to expand in vitro human $\gamma\delta$ T cells. Peripheral blood mononuclear cells were incubated in vitro with different N-BPs derivatives at the indicated final concentrations and 20 U/mL final concentration of rIL-2, for 7 days at 37 °C. At the end of the incubation period, cells were collected and the $\gamma\delta$ T cell expansion factor calculated as described in Experimental Section. (b) Mechanism of action of different N-BPs derivatives on human $\gamma\delta$ T cell activation. Expansion in vitro of $\gamma\delta$ T cells was carried out in the presence or absence of mevastatin or lovastatin, both used at 1 μM final concentration.

in vitro/vivo antitumor activity. Moreover, with the aim of having more lipophilic species and gaining better insight into the SAR of zoledronate, we have additionally synthesized compounds **6b−f**.

Pharmacological Evaluation. All the synthesized compounds have been tested in a preliminary assay for their in vitro bioactivity toward activation−expansion of $\gamma\delta$ T lymphocytes. The capacity of bisphosphonates to activate, in vitro, human $\gamma\delta$ T lymphocytes was studied in comparison to zoledronic acid and phosphostim (**3**), the bromohydrin derivative of isopentenyl pyrophosphate, which strongly activates $\gamma\delta$ T lymphocytes.[16]

Figure 2a and Table 1 report the activity of the compounds toward expansion $\gamma\delta$ T lymphocytes. In particular, Figure 2a shows the results of one typical dose−response experiment out of seven, in which peripheral blood mononuclear cells were stimulated in vitro with different concentrations of compounds and low doses of IL-2 for 7 days. The expansion of $\gamma\delta$ T cells was calculated and expressed as an expansion factor. At first glance, it is evident that activity of the compounds seems strongly influenced by the position of the nitrogen in the aromatic system, with the imidazole derivative **6a** being more active than the pyrazole compound **6b** by more than 5000 times. This is in perfect line with the theory that the protonable nitrogen has to be at a certain distance from the geminal carbon atom of N-BPs to properly mimic the cationic transition intermediate formed during the FPPS catalytic cycle.[15,17] In the in vitro FPPS

Table 1. Bioactivity of Phosphoantigens and N-BPs for Vγ9V δ2 T Lymphocytes

compound	Half-maximun stimulation of Vγ9Vδ2 T lymphocytes (μM)
BrHPP	0.015−0.001
IPP	1−3
Zoledronate	0.1−0.3
6a	0.001−0.003
6b	>10
6c	1−2
6d	>10
6e	0.2−0.4
6f	0.1−0.3

Table 2. Percentage ($\pm$SE[a]) of Apoptosis Induced by 100 μM Compound **6a** and 100 μM Zoledronic Acid

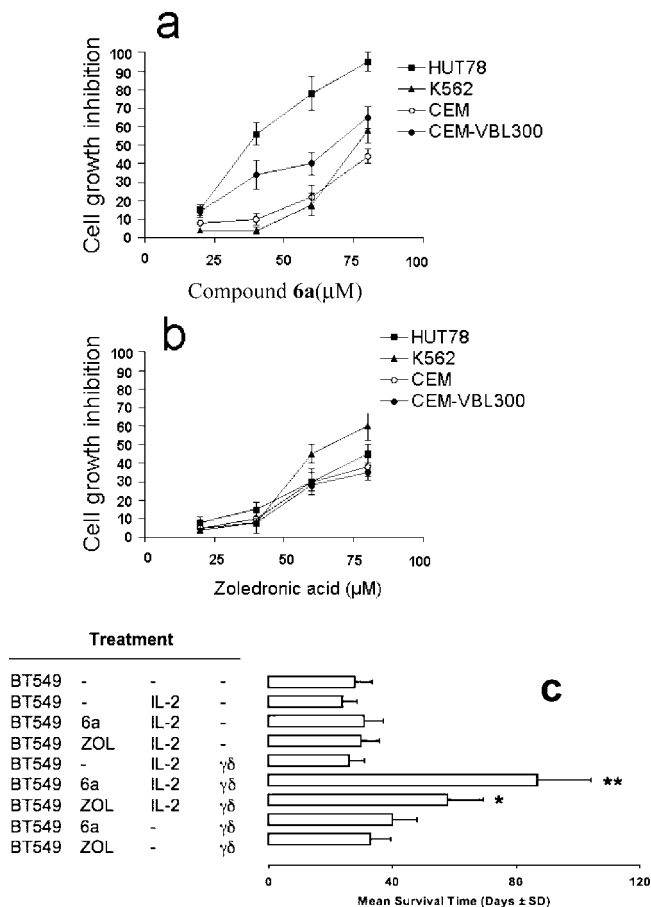|	compound **6a**	zoledronic acid
HUT78	40 ± 5.3	24 ± 4.6
K562	15 ± 3.2	16 ± 5.1
CEM	22 ± 3.1	20 ± 4.4
CEM-VBL300	37 ± 6.0	22 ± 3.2
CFU-GM	15 ± 2.2	18 ± 2.7

[a] SE = standard error.

assays (Table 3), it becomes apparent that movement of the nitrogen away from the position of the nitrogen in zoledronate leads to a large decrease in potency, e.g., **6b**.

Furthermore, the basicity of the nitrogens present in the ring also plays a pivotal role in determining the different pharmacological profiles of the compounds under study, influencing their strength of binding to the enzyme as well as their ability to pass through the cellular membrane. In fact, from the enzyme inhibition assays (Table 3), it clearly emerges that compounds presenting a more basic nitrogen such as **6a**, **6c**, and **6d**, show lower IC$_{50}$ values. This is probably due to a stronger interaction of the protonable nitrogen with the nearby Lys200 and Thr201.

Moreover, although the introduction of purine system **6e**,**f** decreases by around 100-fold, the affinity for the enzyme, those compounds show an activity on human $\gamma\delta$ T cell activation comparable to that of zoledronic acid. It seems likely that their lipophilic character enhances the passing rate thorough the cellular membrane.

However, as summarized in Table 1, the most surprising finding is that the deshydroxyzoledronate **6a** is approximately 100 times more capable of activating $\gamma\delta$ T lymphocytes with respect to zoledronate, considering that the IC$_{50}$ for FPPS inhibition for **6a** is twice that of zoledronate (Table 3). In fact, derivative **6a** was extremely active in inducing activation of human $\gamma\delta$ T lymphocytes upon culture of peripheral blood mononuclear cells (PBMC) in the presence of a low dose (20 U/mL final concentration) of interleukin (IL)-2. Dose response analysis revealed that optimal stimulation and expansion of human $\gamma\delta$ T cells occurs at the final concentration of 1 nM. In addition, **6a** produced a phenotypic switch from naïve and central memory to effector memory cells, the latter exerting important effector functions (such as production of TNF-α and IFN-γ and cytotoxicity) against tumor cell lines in vitro (data not shown).

With regard to the mechanism of action of **6a**, from our initial in vitro studies we found that: (1) as shown in Figure 2b, treatment of PBMC with **6a** and IL-2, but in the presence of mevastatin or lovastatin, blocks the drug effects; (2) when the above-described in vitro assay is carried out with PBMCs depleted of monocytes, the drugs' effects again disappear (data not shown). Both these sets of experiments clearly indicate that **6a** does not act directly on the $\gamma\delta$ T cell receptor but may

Figure 3. (a) Cell growth inhibition induced by different concentration of compound **6a**. (b) Cell growth inhibition induced by different concentration of zoledronic acid. (c) Antitumor effect of **6a** and $\gamma\delta$ T cells in SCID mice in vivo. SCID mice received a single intraperitoneal injection of the breast cancer cell line BT549. Mice concomitantly received with the tumor cells an intraperitoneal injection of human recombinant (r)IL-2, or **6a**, or zoledronate, or **6a** plus rIL-2, or zoledronate plus rIL-2. Where indicated, mice received highly purified human $\gamma\delta$ T cells. For a complete description of cell numbers, drug doses, and time points, see details in Experimental Section. Data show the mean survival time expressed in days. *$p < 0.02$ and **$p < 0.005$, when compared to all other groups.

indirectly affect $\gamma\delta$ T cells via IPP production in monocytes and macrophages, which are ultimately responsible for cell activation and differentiation. It seems likely, therefore, that **6a** behaves like other "third generation" N-BPs, although it proved considerably more potent than zoledronic acid.

To gain better insight into the antitumor activity of **6a**, we further investigated its apoptotic effect on different tumor cell lines and its toxicity on normal and bone marrow-derived hematopoietic cells. The cytotoxic activity of **6a** and of zoledronate was tested on the HUT78 (human T-lymphoma), K562 (chronic myeloid leukemia expressing the antiapoptotic oncogene Bcr-Abl), CCRF-CEM (acute lymphoblastic), CCRF-CEM VBL300 (P-glycoprotein, multiple drug resistant (MDR) protein expressing acute lymphoblastic) cell lines. Interestingly, compound **6a** was endowed with antiproliferative effects and pro-apoptotic activity higher than that of zoledronic acid in both human lymphoma HUT78 cells and P-glycoprotein expressing CCRF-CEM VBL300, while no significant differences were observed in K562 and CCRF-CEM cells (Figure 3a,b). Moreover, compound **6a** showed in HUT78 and CCRF-CEM VBL300 cells a pro-apoptotic activity higher than that of zoledronic acid (Table 2). Of note and quite surprisingly,
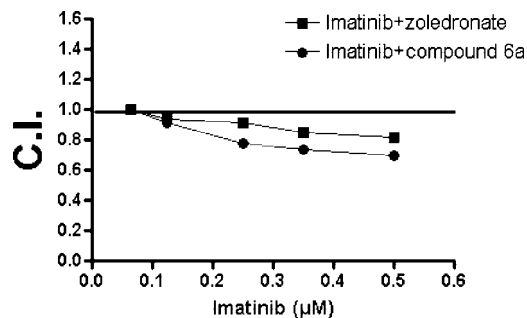
Figure 4. Effects of imatinib−zoledronic acid and imatinib−compound **6a** combinations in K562 cells. Cells were incubated with 30 μM zoledronic acid or 30 μM compound **6a** in combination with concentrations of imatinib ranging from 0.065 to 0.5 μM. After 48 h, the number of living cells was determined and expressed as percentage of control. Combination index (CI) was calculated as described in materials and methods. Combinations were additive when CI = 1, synergistic when CI < 1, and antagonist for CI > 1.

Table 3. Inhibition of Recombinant Human FPPS by N-BP

compound	IC$_{50}$ $\pm$ SEM (nM)
Zoledronate	4.1 ± 0.22[29]
6a	9.03 ± 1.8
6b	3069 ± 264
6c	16.1 ± 1.4
6d	28.1 ± 2.8
6e	388.2 ± 16.2
6f	883.1 ± 71.9

compound **6a** was more active than zoledronic acid in the MDR-expressing cells than in the parental CCRF-CEM line (Figure 3a,b and Table 2). As shown in Figure 3a,b and Table 2, zoledronic acid and **6a** were barely active on Bcr-Abl, expressing K562 cells when used at concentrations lower than 50 μM. On the basis of recent reports indicating that zoledronic acid and imatinib mesilate combination have a synergistic activity on Bcr-Abl expressing cells,[18] we investigated the effects of **6a** in combination with imatinib. K562 cells were exposed to different concentrations of imatinib in combination with 30 μM **6a** or zoledronic acid. Figure 4 shows that imatinib-**6a** combinations display a synergic activity higher than the imatinib−zoledronic acid combination. Additionally, both zoledronic acid and compound **6a** proved to be nontoxic on normal hemopoietic CFU-GM. Therefore, besides the potent activation of Vγ9Vδ2 T lymphocytes, compound **6a** leads to a greater cytotoxic activity than zoledronic acid.

Prompted by these startling results, we decided to test the antitumor effects of **6a** in vivo. We investigated the in vivo tumor reactivity of human $\gamma\delta$ T cells activated and expanded in vitro and then adoptively transferred into SCID mice, according to the experimental protocol described by Kabelitz et al.,[19] analyzing the optimal therapeutic efficacy against the breast cancer BT459 cell line. SCID mice were conditioned by irradiation and antiasialo-GM1 monoclonal antibody treatment, and received at day 0 a single intraperitoneal injection of the breast cancer cell line BT549 (2 $\times$ 10^6/mouse). The high numbers of tumor cells were inoculated to allow for fully fledged tumor growth within the period before graft-vs-host reactions developed in the SCID mouse reconstituted with human lymphocytes. Mice received concomitantly, with the tumor cells, an intraperitoneal injection of human recombinant (r)IL-2 (300 ng), or 6a (2 μg), or zoledronate (5 μg), or **6a** (2 μg) plus rIL-2 (300 ng), or zoledronate (5 μg) plus rIL-2 (300 ng). In addition, mice received highly purified human $\gamma\delta$ T cells (2 $\times$ 10^7/mouse) where indicated. $\gamma\delta$ T cells (2 $\times$ 10^7/mouse) and zoledronate

(5 μg), or **6a** (2 μg), were injected every 15 days, while (r)IL-2 (300 ng) was given on the same day and at 3 and 6 days after each injection of γδ T cells.

As shown in Figure 3c, neither **6a** nor zoledronate or rIL-2, given alone or in combination, improved the survival of the mice. Survival was prolonged when γδ cells where given together with **6a** but not together with zoledronate or IL-2, although the difference (40 ± 10 versus 28 ± 6) was not statistically significant. The application of γδ T cells together with zoledronate and rIL-2 significantly prolonged the mean survival time ($p < 0.02$). Much longer survival was achieved, however, when γδ T cells were given together with **6a** and rIL-2 ($p < 0.005$). Interestingly, the difference in survival between mice receiving γδ T cells + **6a** + rIL-2 and those receiving γδ T cells + zoledronate + rIL-2 was statistically significant ($p < 0.05$), indicating that **6a** is more potent than zoledronate in activating and sustaining the antitumor activity of human γδ T cells.

In conclusion, we have synthesized a small series of N-BPs structurally related to zoledronate, whose antitumor activity has been previously demonstrated, with the aim of improving its in vivo anticancer property. From our research efforts, we identified compound **6a**, which shows a better ability to activate γδ T cell expression and an increased proapoptotic effect compared to the most potent γδ T cells agonist known to date (zoledronate). Moreover, from our in vivo tests, where the antitumor effect of **6a** was studied in the presence of a variety of other agents, we identified a synergic pro-apoptotic activity when it is administered with imatinib mesylate (Gleevec). Thus, taking into account the unique pharmacological profile of **6a**, characterized by a potent activation of γδ T cells, and by a remarkable proapoptotic effect both in vitro and in vivo, it may represent a promising anticancer drug which can be added to the traditional chemotherapy of a wide range of tumor types.

Experimental Section

Molecular Modeling. Docking Simulations. Molecular docking of zoledronate and **6a** into the three-dimensional X-ray structure of FPPS (PDB code: 2F8Z) was carried out using the AutoDock software package (version 4.0) as implemented through the graphical user interface AutoDockTools (ADT 1.4.6).[20]

Ligands and Protein Setup. The structures of the inhibitors were first generated from the standard fragment library of the SYBYL software version 7.3.[21] The docking parametrization of ligands, the cofactor isopentenyl pyrophosphate (IPP), and the region of the enzyme including the metals and its coordinating ligands (Mg subsite) were performed by using the Gaussian03 package[22] by applying a full geometry optimization at Hartree−Fock level of theory and then calculating the charges using the restrained electrostatic potential (RESP) fitting procedure.[23,24] For both the optimization and the electrostatic potential (ESP) calculation, the locally dense 6-31G* basis set was used.

The starting geometry of the Mg subsite for ab initio calculations was derived by a crystallographic template (PDB code: 2F8Z) including the cocrystallized zoledronic acid necessary to get an octahedral coordination of the ions. We treated the three magnesium as ions in the +2 oxidation state and with a low spin state (S = 0).

To properly describe the electrostatic protein environment, the N and C termini of the coordinating aspartates were capped with NME and ACE residues, respectively. Hence, the system was geometrically optimized by constraining the atoms of the backbone of the aspartates and using the previously reported locally dense basis set. The model system was then optimized until reaching the default Gaussian03 convergence criterion.

The RESP charges were then calculated on the geometrically minimized ligands, cofactor, and Mg subsite. First, the ESP were calculated again by means of the Gaussian package and then the

RESP charges were obtained by a two-stages fitting procedure,[25] fitting first the polar areas by using weak hyperbolic restraints (0.0005 au) and then fitting the remaining areas, imposing equivalencies, and by using a stronger hyperbolic restraint (0.001 au). In each step, the charges of the standard residues ACE and NME were constrained to their AMBER force field value.[25] The electrostatic potential used as an input by the RESP program was sampled by adapting the Merz−Singh−Kollman scheme,[26] namely using 10 concentric layers at the default level of spacing, a surface density of 6 points/Å2, and adopting the covalent radius of 0.86 Å for magnesium as reported on the WebElements server (Winter M. WebElements Periodic Table; United Kingdom: University of Sheffield. http://www.webelements.com/). Hence, the computed charges for ligands, cofactor, and Mg subsite were used for further docking calculations.

Docking Setup. The docking area has been defined by a box, centered on the mass center of the cocrystallized zoledronate. Grids points of 40 × 40 × 40 with 0.375 Å spacing were calculated around the docking area for all the ligand atom types using AutoGrid4. For each ligand, 100 separate docking calculations were performed. Each docking calculation consisted of 2.5×10^6 energy evaluations using the Lamarckian genetic algorithm local search (GALS) method. A low-frequency local search according to the method of Solis and Wets was applied to docking trials to ensure that the final solution represents a local minimum. Each docking run was performed with a population size of 150, and 300 rounds of Solis and Wets local search were applied with a probability of 0.06. A mutation rate of 0.02 and a crossover rate of 0.8 were used to generate new docking trials for subsequent generations. The GALS method evaluates a population of possible docking solutions and propagates the most successful individuals from each generation into the next one. The docking results from each of the 100 calculations were clustered on the basis of root-mean square deviation (rmsd = 1.5 Å) between the Cartesian coordinates of the ligand atoms and were ranked on the basis of the free energy of binding.

Chemistry. General Methods and Materials. Melting points were obtained in open capillary tubes and are uncorrected. Reactions and product mixtures were routinely monitored by thin-layer chromatography (TLC) on Merck silica gel precoated F254 plates. Nuclear magnetic resonance (^{1}H NMR, ^{13}C NMR) spectra were determined in CDCl₃ solution unless otherwise indicated with a Bruker AC-200 or with Varian Mercury Plus 400 spectrometer, and peak positions are given in parts per million downfield from tetramethylsilane as the internal standard; J values are expressed in hertz. Compound **6e** has been studied using a Varian Inova 600 MHz spectrometer in D₂O solution. Light petroleum ether refers to the 40−60 °C boiling range fractions. Column chromatography was performed with Merck 60−200 mesh silica gel. All drying operations were performed over anhydrous sodium sulfate. Column chromatography (medium pressure) was carried out using the "flash" technique. Microanalysis of all new synthesized compounds agreed within ±0.4% of calculated values. The microwave reactions were performed in a Discover CEM, which produced controlled irradiation with a power of 0−300 W.

Tetraethyl-ethenylidenebisphosphonate. (4). Paraformaldehyde (520 mg, 17.3 mmol) and diethyl amine (0.36 mL, 3.46 mmol) were combined in 10 mL of methanol, warmed until clear, then treated with tetraethylmethylene bisphosphonate (0.86 mL, 3.46 mmol) and refluxed for 18 h. The mixture was concentrated in vacuo, toluene was then added, and the solvent was evaporated again (2 × 5 mL). The residue was dissolved in toluene (20 mL), treated with *p*-toluensulphonic acid (cat.), and refluxed through a Dean−Stark trap for 18 h. The sample was concentrated in vacuo, dissolved in chloroform (20 mL), washed with water (10 mL), dried, and concentrated in vacuo. The residue oil was used without further purifications for the next reaction. Yellow oil; yield: 90%.

^{1}H NMR δ: 1.17 (t, $J = 7.2$, 12H), 3.90−4.03 (m, 8H), 6.63 (s, 1H), 6.70 (d, $J = 38$, 1H), 7.10 (d, $J = 38$, 1H).^{13}C NMR δ: 14.5, 62.4, 121.8, 148.2.

General Procedures for the Synthesis of Tetraethyl Bisphosphonate 5a−f. Method A. A solution of compounds **a−f** (0.66 mmol) and **4** (200 mg, 0.66 mmol) in THF (10 mL) was kept in a microwave vial and heated to 150−160 °C for 15 min in a scientific microwave oven. After cooling at room temperature, the solvent was evaporated in vacuo, the crude material was dissolved in water (10 mL) and extracted with dichloromethane (2 × 15 mL). The organic layers were collected, dried, filtered, and evaporated. The crude material was purified by flash chromatography on silica gel with dichloromethane−methanol as eluent.

Method B. A mixture of compounds **a−f** (0.66 mmol), **4** (200 mg, 0.66 mmol), and TBD (88 mg, 0.066 mmol) in THF (15 mL) was stirred under reflux for 4 h, the solvent was evaporated in vacuo, and the crude material was dissolved in water (10 mL) and extracted with dichloromethane (2 × 10 mL). The organic layers were collected, dried, filtered, and evaporated. The crude material was purified by flash chromatography on silica gel with dichloromethane−methanol as eluent.

Tetraethyl-[2-(imidazol-1-yl)ethyl]-bisphosphonate (5a). Yield 90%; yellow oil. ^{1}H NMR δ 1.25−1.34 (m, 12H), 2.40−2.85 (m, 1H), 4.05−4.21 (m, 8H), 4.41−4.59 (m, 2H), 6.90 (s, 1H), 7.21 (s, 1H), 7.57 (s, 1H). ^{13}C NMR δ 13.4, 45.3, 48.2, 61.3, 121.7, 126.9, 141.6.

Tetraethyl-[2-(pyrazol-1-yl)ethyl]-bisphosphonate (5b). Yield 79%; yellow oil. ^{1}H NMR δ 1.25−1.32 (m, 12H), 3.16−3.43 (m, 1H), 4.02−4.20 (m, 8H), 4.56−4.73 (m, 2H), 6.17−6.19 (m, 1H), 7.48 (d, $J = 2.0$, 1H), 7.52 (d, $J = 2.0$, 1H).

Tetraethyl-[2-(benzoimidazol-1-yl)ethyl]-bisphosphonate (5c). Yield 71%; yellow oil. ^{1}H NMR δ 1.20−1.33 (m, 12H), 2.45−2.80 (m, 1H), 4.08−4.20 (m, 8H), 4.45−4.60 (m, 2H), 7.30−7.42 (m, 2H), 7.83−7.98 (m, 2H), 8.90 (s, 1H). ^{13}C NMR δ 13.2, 25.3, 34.0, 65.3, 118.4, 125.9, 143.9, 151.5.

Tetraethyl-[2-(imidazol-2-yl-thio)ethyl]-bisphosphonate (5d). Yield 45%; yellow oil. ^{1}H NMR δ 1.24−1.34 (m, 12H), 3.80−3.91 (m, 1H), 4.06−4.28 (m, 8H), 4.36−4.52 (m, 2H), 6.64 (d, $J = 2.0$, 1H), 6.87 (d, $J = 2.0$, 1H), 11.15 (br, 1H).

By means of the procedure utilized, **5e** and **5f** were obtained as inseparable mixtures of regioisomers (ratio 9:1), whose structure was defined by NMR experiments carried out on derivative **6e**.

Tetraethyl-[2-(purin-9-yl)ethyl]-bisphosphonate (5e). Yield 48%; yellow oil. Main isomer: ^{1}H NMR δ 1.19−1.24 (m, 12H), 3.36−3.53 (m, 1H), 4.06−4.16 (m, 8H), 4.75−4.83 (m, 2H), 8.17 (s, 1H), 8.95 (s, 1H), 9.11 (s, 1H). ^{13}C NMR δ 13.3, 44.5, 48.7, 62.0, 133.3, 146.6, 149.6, 150.8, 168.3.

Tetraethyl-[2-(6-chloro-purin-9-yl)ethyl]-bisphosphonate (5f). Yield 50%; yellow oil. Main isomer: ^{1}H NMR δ 1.20−1.24 (m, 12H), 3.35−3.43 (m 1H), 4.01−4.15 (m, 8H), 4.73−4.84 (m, 2H), 8.0 (s, 1H), 8.22 (s, 1H), 8.71 (s, 1H). ^{13}C NMR δ 13.0, 41.5, 44.6, 62.3, 133.3, 146.7, 149.5, 150.8, 152.7.

General Procedures for the Synthesis of Bisphosphonic acid 6a−f. Method A. A solution of **5a−f** (0.25 mmol) in concentrated HCl (3 mL) was stirred under reflux for 3 h and the solvent evaporated in vacuo. The residual solid was recrystallized from H_2O-MeOH to give **6a−f**.

Method B. To an ice-cooled solution of **5a−f** (0.25 mmol) in CCl_4 (5 mL) was added iodotrimethylsilane (0.179 mL, 1.25 mmol) dropwise, and the resulting mixture was stirred below 5 °C for 3 h. The reaction mixture was quenched by adding MeOH (10 mL), and the precipitate was collected and recrystallized by from H_2O-MeOH to give **6a−f** as white or yellow solids.

[2-(Imidazol-1-yl)ethyl]-bisphosphonic acid (6a). Yield 90%; white solid, mp >250 °C dec. ^{1}H NMR (NaOD/D_2O) δ 1.83−1.94 (m, 1H), 4.16−4.24 (m, 2H), 6.73 (s, 1H), 7.09 (s, 1H), 7.57 (s, 1H). ^{13}C NMR (NaOD/D_2O) δ 44.3, 47.0, 120.7, 126.9, 138.8. Anal. ($C_5H_{10}N_2O_6P_2$) C, H, N.

[2-(Pyrazol-1-yl)ethyl]-bisphosphonic acid (6b). Yield 79%; white solid, mp = 199−202 °C. ^{1}H NMR (NaOD/D_2O) δ 2.03−2.24 (m, 1H), 4.27−4.39 (m, 2H), 6.02−6.06 (m, 1H), 7.29 (s, 1H), 7.59 (s, 1H). Anal. ($C_5H_{10}N_2O_6P_2$) C, H, N.

[2-(Benzoimidazol-1-yl)ethyl]-bisphosphonic acid (6c). Yield 67%; white solid, mp >250 °C dec. ^{1}H NMR (NaOD/D_2O) δ

2.20−2.35 (m, 1H), 4.45−4.58 (m, 2H), 7.35−7.42 (m, 2H), 7.83−7.98 (m, 2H), 8.72 (s, 1H). ^{13}C NMR (NaOD/D_2O) δ 25.3, 34.0, 118.4, 125.9, 143.9, 151.5. Anal. ($C_9H_{12}N_2O_6P_2$) C, H, N.

[2-(Imidazol-2-yl-thio)ethyl]-bisphosphonic acid (6d). Yield 40%. ^{1}H NMR (NaOD/D_2O) δ 2.89−2.98 (m, 1H), 3.99−4.06 (m, 2H), 7.01−7.03 (m, 2H). Anal. ($C_5H_{10}N_2O_6P_2S$) C, H, N, S.

[2-(Purin-9-yl)ethyl]-bisphosphonic acid (6e). Yield 55%; yellow solid. Title compound was identified by NMR study present as the main isomer (90%). ^{1}H NMR (D_2O) δ 3.05 (m, 1H), 4.95 (m, 2H), 8.97 (s, 1H), 9.30 (s, 1H), 9.42 (s, 1H). ^{13}C NMR (150.81 MHz, D_2O) δ 42.98, 38.38, 132.42, 140.56, 147.23, 153.35, 154.75.

[2-(Purin-7-yl)ethyl]-bisphosphonic acid was found as minor isomer (10%). ^{1}H NMR (D_2O) δ 2.84 (m, 1H), 4.99 (m, 2H), 9.15 (s, 1H), 9.27 (s, 1H), 9.62 (s, 1H). Anal. ($C_7H_{10}N_4O_6P_2$) C, H, N.

[2-(6-Chloro-purin-9-yl)ethyl]-bisphosphonic acid (6f). Yield 59%; yellow solid. Main isomer: ^{1}H NMR (NaOD/D_2O) δ 2.16−2.32 (m, 1H), 4.32−4.42 (m, 2H), 7.93 (s, 1H), 7.97 (s, 1H). ^{13}C NMR (NaOD/D_2O) δ 41.5, 44.6, 133.3, 146.7, 149.5, 150.8, 152.7. Anal. ($C_7H_9ClN_4O_6P_2$) C, H, N.

Biology. Expansion in Vitro of $\gamma\delta$T Cells. Heparinized blood specimens were collected from 12 healthy volunteers (males, age range 24−46 years), all working at the Dipartimento di Biopatologia e Metodologie Biomediche, University of Palermo, upon informed consent. The study was approved by the ethical committee of the University Hospital. Peripheral blood mononuclear cells were incubated in vitro with different N-BPs or BrHPP (at the indicated final concentrations) and 20 U/mL final concentration of rIL-2, for 7 days at 37 °C. At the end of the incubation period, cells were collected and the $\gamma\delta$ T cell expansion factor calculated according to our previously published method.[27]

Expansion in vitro of $\gamma\delta$ T cells, when the mechanism of action of different N-BPs was evaluated, was performed as indicated previously, except that the assay was carried out in the presence or absence of mevastatin or lovastatin, both used at 1 μM final concentration.

In Vivo Antitumor Activity. In vivo antitumor activity of $\gamma\delta$ T cells was evaluated in SCID mice, using the protocol described by Kabelitz et al., with minor modifications.[19]

Briefly, SCID mice (6 mice per group) were conditioned by irradiation (300 rads from a cesium source) and antiasialo-GM1 monoclonal antibody (BD Bioscience) treatment. Mice received at day 0 a single intraperitoneal injection of the breast cancer cell line BT549 (2 × 10^6/mouse). These high numbers of tumor cells were inoculated to allow for full-fledged tumor growth within the period before graft-vs-host reactions developed in the SCID mouse reconstituted with human lymphocytes. Mice received, concomitantly with the tumor cells, an intraperitoneal injection of human recombinant (r)IL-2 (300 ng), or **6a** (2 μg), or zoledronate (5 μg), or **6a** (2 μg) plus rIL-2 (300 ng), or zoledronate (5 μg) plus rIL-2 (300 ng). Where indicated, mice received, in addition, highly purified human $\gamma\delta$ T cells (2 × 10^7/mouse). $\gamma\delta$ T cells (2 × 10^7/mouse) and zoledronate (5 μg), or **6a** (2 μg), were injected again every 15 days, while (r)IL-2 (300 ng) was given on the same day and at 3 and 6 days after each injection of $\gamma\delta$ T cells. *$p < 0.02$ and **$p < 0.005$, when compared to all other groups.

Cytotoxicity Assays. To evaluate the number of live and dead neoplastic cells, the cells were stained with trypan blue and counted on a hemocytometer. To determine the growth inhibitory activity of the drugs tested, 2 × 10^5 cells were plated into 25 mm wells (Costar, Cambridge, UK) in 1 mL of complete medium and treated with different concentrations of each drug. After 48 h of incubation, the number of viable cells was determined and expressed as the percentage of control proliferation.

Clonal Assays. To evaluate the cytotoxic effects of biphosphonates on normal hemopoietic progenitor cells, a clonal assay for CFU-GM (colony-forming units−granulocyte macrophage) was performed. Bone marrow mononucleated cells were obtained from bone marrow aspirates of five normal volunteers. Bone marrow (3−5 mL) was diluted in RPMI 1640, layered over a Ficoll−Hypaque gradient (density, 1.077), centrifuged at 400g for 30 min, and the interface mononuclear cells were collected. The interface cells were

washed three times in PBS, counted, and resuspended at a concentration of 1×10^5 in MEM containing 0.9% methylcellulose, 30% FCS, 10^{-4} M β-mercaptoethanol, 5% medium conditioned by leukocytes in the presence of phytohemagglutinin (PHA-LCM) in 15 mm plastic dishes. After 7 days of culture at 37 °C in an environment of 5% CO_2 and 100% humidity, the number of CFU-GM was evaluated.

Morphological Evaluation of Apoptosis and Necrosis. Drug-induced apoptosis and necrosis was determined morphologically after labeling with acridine orange and ethidium bromide. Cell (2×10^5) was centrifuged (300g) and the pellet was resuspended in 25 μL of the dye mixture. Ten μL of the mixture was examined in oil immersion with a 100$\times$ objective using a fluorescence microscope. Live cells were determined by the uptake of acridine orange (green fluorescence) and exclusion of the ethidium bromide (red fluorescence) stain. Live and dead apoptotic cells were identified by the perinuclear condensation of chromatin, stained by acridine orange (100 μg/ml) or ethidium bromide (100 μg/mL), respectively, and by the formation of apoptotic bodies. The percentage of apoptotic cells was determined after counting at least 300 cells.

Determination of Apoptosis by Annexine-V. Cells (1×10^6) were washed with PBS and centrifuged at 200g for 5 min. Cell pellet was suspended in 100 μL of a staining solution, containing FITC-conjugated Annexine-V and propidium iodide (Annexine-V-Fluos Staining Kit, Roche Molecular Biochemicals, Mannheim, Germany) and incubated for 15 min at 20 °C. The percentage of Annexine-V-positive cells was evaluated by flow cytometry (Becton Dickinson).

Determination of Drug Interactions. For the determination of the interactions between the drugs, the fractional product methods of Webb was applied.[28] The predicted values (c) were calculated according to the equation $c = a \times b/100$, where a and b indicate cell survival values with single agents. Hence, the combination index (CI) was calculated as the ratio between the survival observed with the combinations and the predicted values. The equations CI = 1, CI < 1, and CI > 1 indicate additive effects, synergism, and antagonism, respectively.

Determination of Inhibition of FPP Synthase. FPP synthase was purified and assayed as previously described by Kavanagh et al.[29] Briefly, an expression construct encoding human FPPS (gi 61680822) as N-terminally His$_6$-tagged fusion protein with a TEV cleavage site was expressed in *Escherichia coli* BL21(DE3). Cells were lysed using a high pressure cell disruptor, and the protein was purified to apparent homogeneity using Ni-NTA resin (Qiagen). Gel filtration chromatography was then performed using a Superdex 200 column (GE/Amersham). For analysis of inhibition, 40 ng (1 pmol) of pure FPP synthase was preincubated with N-BP in a volume of 80 μL buffer containing 50 mM Tris pH7.7, 2 mM MgCl$_2$, 0.5 mM TCEP, 20 μg/mL BSA for 10 min. Reactions were started by the addition of 20 μL of 5$\times$ substrate (50 μM GPP and 50 μM 14C-IPP, 400 KBq/μmol) in water, bringing the inhibitor and substrate to the final desired concentrations, and allowed to proceed for an appropriate period of time at 37 °C. Reactions were timed such that a maximum of 10% of the available substrate was used. Assays were terminated by the addition of 0.2 mL of conc HCl/methanol (1:4) and incubated for 10 min at 37 °C. The reaction mixtures were then extracted with 0.4 mL of scintillation fluid Microscint E (Perkin-Elmer). After thorough mixing, the tubes were briefly centrifuged to separate the two phases and the radioactivity was then counted directly using a Microbeta (Perkin-Elmer) scintillation counter. All data were fitted to kinetic models using Graphpad Prism.

Supporting Information Available: Elemental analysis for derivatives **6a–f**. This material is available free of charge via the Internet at http://pubs.acs.org.

References

(1) (a) Russell, R. G. G.; Rogers, M. J. Bisphosphonates: from the laboratory to the clinic and back again. *Bone* **1999**, *25*, 97–105. (b) Takeuchi, M.; Sakamoto, S.; Kawamuki, K.; Kurihara, H.; Nakahara, H.; Isomura, Y. Studies on novel bone resorption inhibitors. Synthesis and pharmacological activities of fused aza-heteroarylbisphosphonate derivatives. *Chem. Pharm. Bull.* **1998**, *46*, 1703–1709.

(2) (a) Martin, M. B.; Grimley, J. S.; Lewis, J. C.; Heat, H. T.; Bailey, B. N.; Kendrick, H.; Yardley, V.; Caldera, A.; Lira, R.; Urbina, J. A.; Moreno, S. N. J.; Docampo, R.; Croft, S. L.; Oldfield, E. Bisphosphonates inhibit the growth of *Trypanosoma brucei, Trypanosoma cruzi, Leishmania donovani, Toxoplasma gondii,* and *Plasmodium falciparum*: a potential route to chemotherapy. *J. Med. Chem.* **2001**, *44*, 909–916. (b) Subhash, G.; Chan, J. M. W.; Lea, C. R.; Meints, G. A.; Lewis, J. C.; Tovian, Z. S.; Flessner, R. M.; Loftus, T. C.; Bruchhaus, I.; Kendrick, H.; Croft, S. L.; Kemp, R. G.; Kobayashi, S.; Nozaki, T.; Oldfield, E. Effects of bisphosphonates on the growth of *Entamoeba histolytica* and *Plasmodium* species in vitro and in vivo. *J. Med. Chem.* **2004**, *47*, 175–187. (c) Hudock, M. P.; Sanz-Rodriguez, C. E.; Song, Y.; Chan, J. M. W.; Zhang, Y.; Odeh, S.; Kosztowski, T.; Leon-Rossell, A.; Concepciòn, J. L.; Yardley, V.; Croft, S. L.; Urbina, J. A.; Oldfield, E. Inhibition of *Trypanosoma cruzi* hexokinase by bisphosphonates. *J. Med. Chem.* **2006**, *49*, 215–223.

(3) (a) Sheares, B. T.; White, S. S.; Molowa, D. T.; Chan, K.; Ding, V. D.; Kroon, P. A.; Bostedor, R. G.; Karkas, J. D. Cloning, analysis, and bacterial expression of human farnesyl pyrophosphate synthetase and its regulation in Hep G2 cells. *Biochemistry* **1989**, *28*, 8129–8135. (b) Tarshis, L. C.; Yan, M.; Poulter, D.; Sacchettini, J. C. Crystal structure of recombinant farnesyl diphosphate synthase at 2.6 Å resolution. *Biochemistry* **1994**, *33*, 10871–10877.

(4) Cheng, F.; Oldfield, E. Inhibition of isoprene biosynthesis pathway enzymes by phosphonates, bisphosphonates, and diphosphates. *J. Med. Chem.* **2004**, *47*, 5149–5158.

(5) Green, J. R. Antitumor effects of bisphosphonates. *Cancer* **2003**, *97* (3 Suppl), 840–847.

(6) Clèzardin, P.; Ebetino, F. H.; Fournier, P. G. J. Bisphosphonates and cancer-induced bone disease: beyond their antiresorptive activity. *Cancer Res.* **2005**, *65*, 4971–4974.

(7) (a) Anderson, K. C.; Kyle, R. A.; Dalton, W. S.; Landowski, T.; Shain, K.; Jone, R.; Hazlehurst, L.; Berenson, J. Multiple myeloma: new insights and therapeutic approaches. *Hematology* **2000**, 166–179. (b) Schultze, J. L.; Nadler, L. M. T cell mediated immunotherapy for B cell lymphoma. *J. Mol. Med.* **1999**, *77*, 322–331. (c) Smyth, M. J.; Godfrey, D. I.; Trapani, J. A. A fresh look at tumor immunosurveillance and immunotherapy. *Nat. Immunol.* **2001**, *2*, 293–299. (d) Groh, V.; Steinle, A.; Bauer, S.; Spies, T. Recognition of stress-induced MHC molecules by intestinal epithelial $\gamma\delta$ T cells. *Science* **1998**, *279*, 1737–1740.

(8) (a) Feldman, E. J.; Brandwein, J.; Stone, R.; Kalaycio, M.; Moore, J.; O'Connor, J.; Wedel, N.; Roboz, G. J.; Miller, C.; Chopra, R.; Jurcic, J. C.; Brown, R.; Ehmann, W. C.; Schulman, P.; Frankel, S. R.; De Angelo, D.; Scheinberg, D. Phase III randomized multicenter study of a humanized anti-CD33 monoclonal antibody, lintuzumab, in combination with chemotherapy, versus chemotherapy alone in patients with refractory or first-relapsed acute myeloid leukemia. *J. Clin. Oncol.* **2005**, *23*, 4110–4116. (b) Linck, D.; Lentini, G.; Tiemann, M.; Fauser, A. A.; Parwaresch, R.; Basara, N. Sequential application of chemotherapy and monoclonalCD20 antibody: successful treatment of advanced composite-lymphoma. *Leuk. Lymphoma* **2005**, *46*, 285–288.

(9) (a) Widler, L.; Jaeggi, K. A.; Glatt, M.; Muller, K.; Bachmann, R.; Bisping, M.; Born, A.; Cortesi, R.; Guiglia, G.; Jeker, H.; Klein, R.; Ramseier, U.; Schmid, J.; Schreiber, G.; Seltenmeyer, Y.; Green, J. R. Highly potent geminal bisphosphonates. From pamidronate disodium (Aredia) to zoledronic acid (Zometa). *J. Med. Chem.* **2002**, *45*, 3721–3738. (b) Fleisch, H.; Russell, R. G.; Francis, M. D. Diphosphonates inhibit hydroxyapatite dissolution in vitro and bone resorption in tissue culture and in vivo. *Science* **1969**, *165*, 1262–1264. (c) Fleisch, H. Bisphosphonates: mechanism of action. *Endocr. Rev.* **1998**, *19*, 80–100.

(10) Rogers, M. J.; Frith, J. C.; Luckman, S. P.; Coxon, F. P.; Benford, H. L.; Monkonnen, J.; Auriola, S.; Chilton, K. M.; Russell, R. G. Molecular mechanisms of action of bisphosphonates. *Bone* **1999**, *24*, 73S–79S.

(11) (a) Morita, C. T.; Jin, C.; Sarikonda, G.; Wang, H. Nonpeptide antigens, presentation mechanism, and immunological memory of human Vγ2Vδ2 T cells: discriminating friend from foe through the recognition of prenyl pyrophosphate antigens. *Immunol. Rev.* **2007**, *215*, 59–76. (b) Hosfield, D. J.; Zhang, Y.; Dougan, D. R.; Broun, A.; Tari, L. W.; Swanson, R. V.; Finn, J. Structural basis for bisphosphonate-mediated

inhibition of isoprenoid biosynthesis. *J. Biol. Chem.* **2004**, *279*, 8526–8529.

(12) Wilhem, M.; Kunzmann, V.; Eckstein, S.; Reiner, P.; Weissinger, F.; Ruediger, T.; Tony, H. γδ T-cells for immune therapy of patients with lymphoid malignancies. *Blood* **2003**, *102*, 200–206.

(13) Dieli, F.; Gebbia, N.; Poccia, F.; Caccamo, N.; Montesano, C.; Fulfaro, F.; Arcara, C.; Valerio, M. R.; Meraviglia, S.; Di Sano, C.; Sireci, G.; Salerno, A. Induction of γδ T-lymphocyte effector functions by bisphosphonate zoledronic acid in cancer patients in vivo. *Blood* **2003**, *102*, 2310–2311.

(14) Dieli, F.; Vermijlen, D.; Fulfaro, F.; Caccamo, C.; Meraviglia, S.; Cicero, G.; Roberts, A.; Buccheri, S.; D'Asaro, M.; Gebbia, N.; Salerno, A.; Eberl, M.; Hayday, A. C. Targeting human γδT cells with zoledronate and interleukin-2 for immunotherapy of hormone-refractory prostate cancer. *Cancer Res.* **2007**, *67*, 7450–7457.

(15) Zhang, Y.; Hudock, M. P.; Krysiak, K.; Cao, R.; Bergan, K.; Yin, F.; Leon, A.; Oldfield, E. Activity of sulfonium bisphosphonates on tumor cell lines. *J. Med. Chem.* **2007**, *50*, 6067–6079.

(16) Espinosa, E.; Belmant, C.; Pont, F.; Luciani, B.; Poupot, R.; Romagne, F.; Brailly, H.; Bonneville, M.; Fournié, J. J. Chemical synthesis and biological activity of bromohydrin pyrophosphate, a potent stimulator of human γδ T cells. *J. Biol. Chem.* **2001**, *276*, 18337–18344.

(17) Rondeau, J. M.; Bitsch, F.; Bourgier, E.; Geiser, M.; Hemming, R.; Kroemer, M.; Lehmann, S.; Ramage, P.; Rieffel, S.; Strauss, A.; Green, J. R.; Jahnke, W. Structural basis for the exceptional in vivo efficacy of bisphosphonate drugs. *ChemMedChem.* **2006**, *1*, 267–273.

(18) Kuroda, J.; Kimura, S.; Segawa, H.; Kobayashi, Y.; Yoshikawa, T.; Urasaki, Y.; Ueda, T.; Enjo, F.; Tokuda, H.; Ottmann, O. G.; Maekawa, T. The third-generation bisphosphonate zoledronate synergistically augments the anti-Ph+ leukemia activity of imatinib mesylate. *Blood* **2003**, *102*, 2229–35.

(19) Kabelitz, D.; Wesch, D.; Pitters, E.; Zöller, M. Characterization of tumor reactivity of human Vγ9Vδ2 γδ T cells in vitro and in SCID mice in vivo. *J. Immunol.* **2004**, *173*, 6767–6776.

(20) (a) Morris, G. M.; Goodsell, D. S.; Halliday, R. S.; Huey, R.; Hart, W. E.; Belew, R. K.; Olson, A. J. Automated Docking Using a Lamarckian Genetic Algorithm and Empirical Binding Free Energy Function. *J. Comput. Chem.* **1998**, *19*, 1639–1662. (b) Huey, R.; Morris, G. M.; Olson, A. J.; Goodsell, D. S. A Semiempirical Free Energy Force Field with Charge-Based Desolvation. *J. Comput. Chem.* **2007**, *28*, 1145–1152.

(21) *SYBYL 7.3, Molecular Modeling System*; Tripos Inc.: St. Louis, MO.

(22) Frisch, M. J.; Trucks, G. W.; Schlegel, H. B.; Scuseria, G. E.; Robb, M. A.; Cheeseman, J. R.; Montgomery, J. A., Jr.; Vreven, T.; Kudin, K. N.; Burant, J. C.; Millam, J. M.; Iyengar, S. S.; Tomasi, J.; Barone, V.; Mennucci, B.; Cossi, M.; Scalmani, G.; Rega, N.; Petersson, G. A.; Nakatsuji, H.; Hada, M.; Ehara, M.; Toyota, K.; Fukuda, R.; Hasegawa, J.; Ishida, M.; Nakajima, T.; Honda, Y.; Kitao, O.; Nakai, H.; Klene, M.; Li, X.; Knox, J. E.; Hratchian, H. P.; Cross, J. B.; Bakken, V.; Adamo, C.; Jaramillo, J.; Gomperts, R.; Stratmann, R. E.; Yazyev, O.; Austin, A. J.; Cammi, R.; Pomelli, C.; Ochterski, J. W.; Ayala, P. Y.; Morokuma, K.; Voth, G. A.; Salvador, P.; Dannenberg, J. J.; Zakrzewski, V. G.; Dapprich, S.; Daniels, A. D.; Strain, M. C.; Farkas, O.; Malick, D. K.; Rabuck, A. D.; Raghavachari, K.; Foresman, J. B.; Ortiz, J. V.; Cui, Q.; Baboul, A. G.; Clifford, S.; Cioslowski, J.; Stefanov, B. B.; Liu, G.; Liashenko, A.; Piskorz, P.; Komaromi, I.; Martin, R. L.; Fox, D. J.; Keith, T.; Al-Laham, M. A.; Peng, C. Y.; Nanayakkara, A.; Challacombe, M.; Gill, P. M. W.; Johnson, B.; Chen, W.; Wong, M. W.; Gonzalez, C.; Pople, J. A. *Gaussian 03*; Gaussian, Inc.: Pittsburgh, PA, 2003.

(23) Bayly, C. I.; Cieplak, P.; Cornell, W. D.; Kollman, P. A. A well-behaved electrostatic potential based method using charge restraints for determining atom-centered charges: the RESP model. *J. Phys. Chem.* **1993**, *97*, 10269–10280.

(24) Cornell, W. D.; Cieplak, P.; Bayly, C. I.; Kollman, P. A. Application of RESP charges to calculate conformational energies, hydrogen bond energies, and free energies of solvation. *J. Am. Chem. Soc.* **1993**, *115*, 9620–9631. (b) Bayly, C. I.; Cieplak, P.; Cornell, W. D.; Kollman, P. A. A well-behaved electrostatic potential based method using charge restraints for determining atom-centered charges: the RESP model. *J. Phys. Chem.* **1993**, *97*, 10269–10280.

(25) Cornell, W. D.; Cieplak, P.; Bayly, C. I.; Gould, I. R.; Merz, K. M.; Ferguson, D. M.; Spellmeyer, D. C.; Fox, T.; Caldwell, J. W.; Kollman, P. A. A second generation force field for the simulation of proteins, nucleic acids, and organic molecules. *J. Am. Chem. Soc.* **1995**, *117*, 5179–5197.

(26) (a) Singh, U. C.; Kollman, P. A. An approach to computing electrostatic charges for molecules. *J. Comput. Chem.* **1983**, *5*, 129–145. (b) Besler, B. H.; Merz, K. M.; Kollman, P. A. Atomic charges derived from semiempirical methods. *J. Comput. Chem.* **1990**, *11*, 431–439.

(27) Dieli, F.; Gebbia, N.; Poccia, F.; Caccamo, N.; Montesano, C.; Fulfaro, F.; Arcara, C.; Valerio, M. R.; Meraviglia, S.; Di Sano, C.; Sireci, G.; Salerno, A. Induction of γδ T-lymphocyte effector functions by bisphosphonate zoledronic acid in cancer patiens in vivo. *Blood* **2003**, *102*, 2310–2311.

(28) Webb, J. L. Effect of more than one inhibitor. In: *Enzymes and Metabolic Inhibitors*; Academic Press: New York, 1966; pp 66−79.

(29) Kavanagh, K. L.; Guo, K.; Dunford, J. E.; Wu, X.; Knapp, S.; Ebetino, F. H.; Rogers, M. J.; Russell, R. G.; Oppermann, U. The molecular mechanism of nitrogen-containing bisphosphonates as antiosteoporosis drugs. *Proc. Natl. Acad. Sci. U.S.A.* **2006**, *103* (20), 7829–7834.